NASA GODDARD SPACE FLIGHT CENTER

PREP II PROGRAM WRITTEN REPORT

Design and Fabrication of a Sub-K Cooling System for the EXCLAIM Project

Jacob S. Nellis Cryogenics and Fluids Branch (552) Instrument Systems and Technology Directorate

Subject Matter Expert
Dr. Mark Kimball
Mentor
Dr. Amir Jahromi

Supervisor's
Dr. Eric Silk
Dr. Paul Rueger
Principle Investigator
Dr. Eric Switzer

Abstract

The Experiment for Cryogenic Large-Aperture Intensity Mapping (EXCLAIM) is a balloon-borne telescope designed to investigate the dramatic drop in star formation in the Universes recent past (red-shift $0 \le z \le 2.5$). EXCLAIM achieves high sensitivity using a cryogenic telescope coupled to six integrated spectrometers and employing kinetic inductance detectors (KID) [1].

For accurate science measurements, the focal plane array (FPA) requires cooling to 100 mK. This is accomplished via a three-stage continuous adiabatic demagnetization refrigerator (CADR), backed by a 4He adsorption refrigerator. The receiver and telescope are submerged in a dewar of liquid helium to maintain a heat sink at 1.7K. To prepare for a fall 2023 science flight, the 3 stage CADR was designed, built, and tested from 08/21 - 12/22, using a combination of both novel and heritage designs, borrowing components from the previous PIPER balloon mission. This report describes the development life-cycle of EXCLAIM's Sub-K cooling system with an emphasis on the 3 stage CADR.

core in-house competency for these missions [3]. These systems are comprised of a para-magnetic salt, surrounded by a coil of superconducting wire that generates strong magnetic fields. The design takes advantage of the magneto-caloric effect to provide cooling. These systems have the advantage of being smaller than dilution refrigerators, and additionally have no moving parts. The main drawback however, is that the salt pill needs to be warmed to a reject temperature in order to re-magnetize the pill. Heat switches are connected to the salt pill to thermally connect or disconnect the pathway to the heat sink as required [4]. This limits the time that detectors can be used while the ADR recycles. In 1998, the Cryogenics and Fluids branch expanded on this concept to develop a continuous ADR [3]. This was done by using multiple ADR stages, allowing certain stages to provide cooling, while subsequent stages recycle. This allows the FPA to be kept at a constant 100mK throughout the telescopes operation.

1 Introduction

Detector arrays have provided revolutionary sensitivity for surveys across the electromagnetic spectrum [2]. However, due to their sensitivity, radiation from parasitic heat internal to the telescope can cause excess noise. For this reason, the focal plane array needs to be maintained at 100mK to achieve optimal performance.

Goddard Space Flight Center (GSFC) has a history of using Sub-K cooling on projects. From the 1970's to 2000, ADR's were developed as a

The Primordial Inflation Polarization Explorer (PIPER), was a recent balloon borne project that employed a four stage CADR to achieve Sub-K cooling. In 2017, PIPER underwent an engineering test flight that ended in a 'crash landing'. This caused damages to the CADR, which was subsequently replaced for PIPER's science flight. EXCLAIM has similar design constraints to PIPER, and upon initial inspection of the damaged CADR in 2020, a plan was proposed to refurbish the CADR for use in EXCLAIM.

2 Design Overview

2.1 Operational Environment

The EXCLAIM gondola is 10'x12'x15' and operates at an altitude of 27 km. The gondola houses a LHe bath and an optics receiver assembly that is partially submerged in this bath. The LHe bath progressively cools the receiver from 6K to 1.7 K as the atmosphere acts as a natural pump. Primary and secondary lenses sit above this bath and direct photons into the FPA housed at the bottom of the receiver assembly. The FPA is suspended with carbon fiber tubes connected to a copper ring that is maintained at 900 mK. The CADR and RF ring are also cooled to 900mK via an adsorption refrigerator. The CADR then provides the remaining cooling power necessary to pull the FPA from 900mK to its operating temperature at 100mK. Figure 1 shows the general layout of these components.

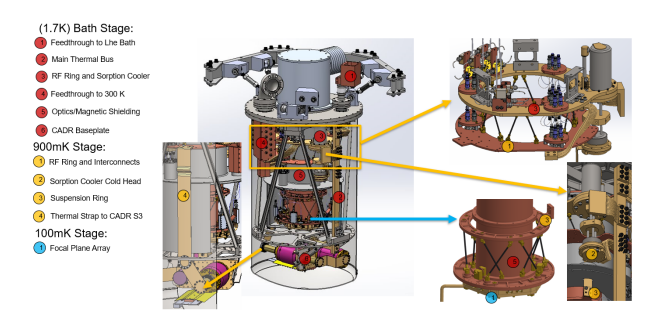


Figure 1: Receiver Design Assembly. Receiver consists of three main thermal sections. CADR is housed at bottom of Receiver, directly below FPA.

2.2 CADR Design

While PIPER employed four ADR stages, and rejected its heat to the 1.7 K bath temperature,

EXCLAIM will only need three stages, as we are able to reject to the 900mK RF ring. Figure 2 shows the configuration of the ADR when integrated into EXCLAIM's receiver.

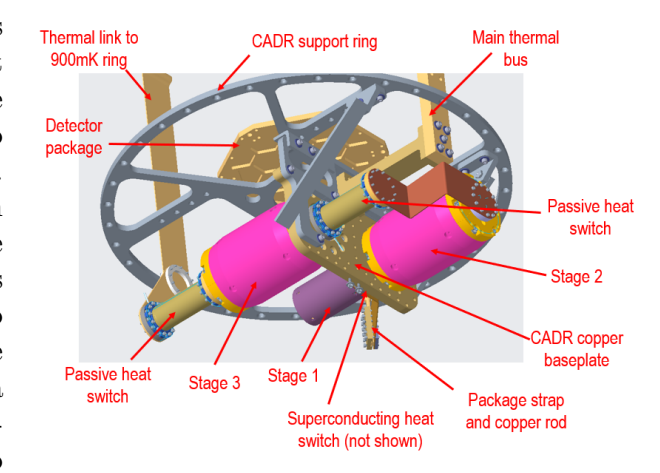


Figure 2: CADR CAD Model. Stage and heat switch designs are from PIPER. CADR baseplate, orientation and configuration are novel for EXCLAIM. Stages are ordered sequentially from coldest to warmest.

The para-magnetic salt in these ADR stages is chromium potassium alum (CPA), and they are suspended from the base plate with Kevlar suspensions to limit parasitic heating. Two passive gas-gap heat switches (PGGHS) are used to isolate stage 2 from stage 3, and stage 3 from the 900 mK ring. A superconducting heat switch (SCHS) is used to isolate stage 1 from stage 2. The properties of each stage are summarized in Table 1, and the properties of the heat switches are summarized in Table 2. These components are discussed in depth in the Fabrication and Refurbishment sections.

Table 1: Stage Properties

Stage	Max Current	Operating Temps
1	800 mA	100 mK
2	2.5 A	70 mK - 330 mK
3	4 A	280 mK - 1 K

Table 2: Heat Switch Properties

Name	Type	On/Off Temperatures
HS 3/bp	PGGHS	Off below 1 K
HS 2/3	PGGHS	Off below 250 mK
HS 1/2	SCHS	Off $I = 250 \text{ mA}$

The copper base-plate was redesigned to accommodate the new locations of the thermal connections to the FPA and heat sink. This plate connects to the main thermal bus, and is suspended with stainless steel brackets to the horizontal support plate sitting between the CADR and FPA. The horizontal support plate was redesigned to reduce mass by 25% while still meeting factor of safety requirements under 8g loading conditions set forth by the Columbia Scientific Balloon Facility (CSBF).

The straps in this design are 1 mm thick and 38 mm wide. These straps and the base plate are gold plated to increase joint conductance between mated surfaces. The shields surrounding stages 2 and 3 are made from Silicon Iron A-FM material and are 0.3" thick. A model was made to simulate the magnetic fields at the FPA generated by the ADR magnets, and showed these shields provide adequate protection to limit the FPA from seeing fields \geq 5 Gauss, which is a design requirement.

2.3 Thermal Design Requirements

EXCLAIM requires the sub-Kelvin cooling system to maintain a 100mK temperature for 4 hours (threshold) up to 12 hours (goal). Since the CADR runs continuously, the component that will limit hold time is the adsorption cooler. This cooler has 28 J of cooling capacity after a 2 hour recycle, and will be recycled immediately before the science operation starts. Thus, the hold time can be estimated by calculating the heat rate to the adsorption cooler throughout the mission.

Initially, after the adsorption cooler recycles, the receiver will be sitting at 1.7 K. The adsorption cooler will be responsible for initially cooling the CADR and FPA from 1.7 K to 900 mK, and the CADR will then be responsible for pulling the FPA down to its final operating temperature of 100 mK. A python script was made to model and calculate the sum of heat capacities and determined that 0.8 J will be used by the adsorption cooler for the initial cool down.

To determine if the CADR will be able to pull the FPA down to its operating temperature, Eq. (1) to used to determine that there is enough entropy capacity in the CADR. This calculation showed that the entropy capacity in the CADR is about equal to the entropy that needs to be lifted (1.03 and 0.93 J/K respectively). This is an issue, as there appears to be no design margins to account for any unexpected increases in heat capacity. One solution to this is to use what is known as 'bootstrapping'. This is when the coldest stage is cooled below its SCHS temperature to isolate it and the FPA from stages 2 and 3, this allows them to recycle and gain additional entropy capacity, but has the drawback of taking longer to reach operating temperature. This mechanism will be tested during the integration/testing campaign using a heater initially, and a dummy mass during final testing. Figure 3 shows the bootstrapping operation being performed during the PIPER testing campaign.

$$\sum \Delta S_{stage}(B_{high} \to B_{low}) \ge \sum \int_{T_l}^{T_h} \frac{CdT}{T_{salt}(T)}$$
(1)

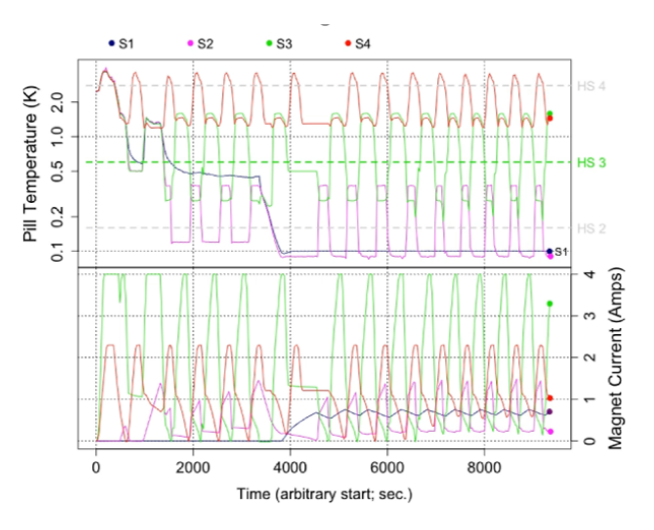


Figure 3: PIPER Bootstrapping Data. Plot shows Stage 1 initially get pulled below the heat switch temperature, effectively isolating it and the FPA from the rest of the CADR. This is what allows the bootstrapping to take place. Stages 2 and 3 recycle until they have enough capacity to finish pulling stage 1 to its operating temperature.

2.4 Steady State Operation

When the warmest stage of the CADR is providing cooling (not rejecting to the adsorption cooler), the base loading on the adsorption cooler

is estimated to be 39 μ W. The ADR will reject an additional 1.12 J of heat to the cooler each time it recycles. Cycling the ADR quickly will drastically reduce hold time, as it will not only provide more heat to the adsorption cooler, but it will also increase the heat sink temperature that it is rejecting to. This results in an increase in the parasitic heat entering the FPA. Figure 4 shows the temperature of the adsorption cooler as cycle time decreases.

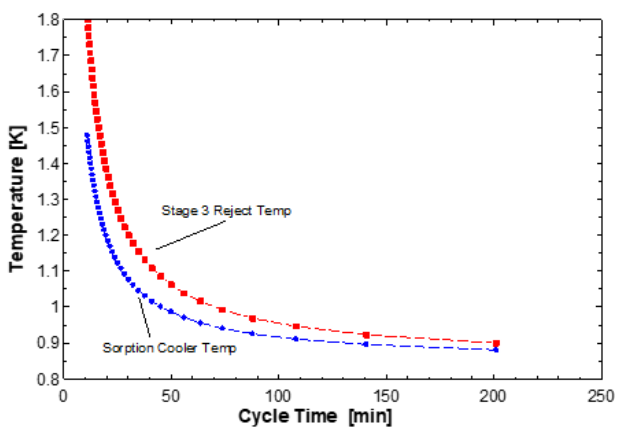


Figure 4: Adsorption Cooler Temperature and CADR Reject Temperature vs. Cycle Time

A model was made to simulate the operating conditions of the CADR, and calculate the maximum amount of heat lift that stage 1 is capable of for different cycle times. This result was compared to the calculated parasitic heat entering the FPA. The maximum cycle time can then be defined as the point where stage 1's cooling power is equal to the cooling power required. This plot is shown in Figure 5. The maximum cycle time was determined to be 108 minutes.

Subtracting the initial cooling required to start operation from the 28 J of initial cooling capacity provided by the adsorption refrigerator, we end up with 25.9 J remaining for sci-

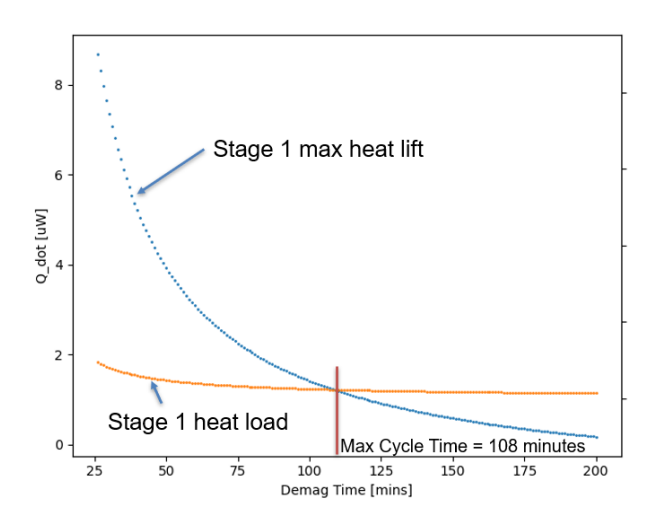


Figure 5: Stage 1 heat lift compared to parasitic loading. The intersection of these lines indicates the point that Stage 1 will not be able to keep up with the parasitic heating.

ence operation. With the calculated heat rate of $\frac{1.12J}{108min/cyc}$ the hold time is greater than 40 hours. This gives us a factor of 4 margin on the hold time requirements.

In addition to this model, a transient implicit numerical model was created to simulate different design conditions in real time and compare with lab data. This model allows the stages to be controlled with PID loops, and has an interface similar to the interface used in our data acquisition system. This software has expanded beyond the scope of EXCLAIM and is being further refined to allow for custom CADR designs, allowing it to be used on any CADR project in the future.

3 Fabrication and Refurbishment

3.1 Magnet Winding

Stages 1 and 2, along with the SCHS each required new superconducting magnets which had to be wound. Table 3 shows the wire requirements for each stage.

Table 3: Wire Specs

Part	Supercon Wire	Num. Windings
1	T48B-BM	4,603
2	15S40	15,000
SCHS	382BM	6,448

These new magnets are produced by first applying a thin layer of Kapton tape to the mandrel; this is done insulate the wire from the metal mandrel and assist in preventing shorts. The wire is wound whilst simultaneously applying CTD-521 epoxy onto the mandrel. This is to fix the windings in place once the epoxy cures.

Stage 1 is not suspended from its magnet, this is not required since the hysteresis heating from the magnet is relatively low. This made the removal of the old magnet particularly difficult while preserving the salt pill inside during the process. The old magnet was removed by attaching the stage to a lathe and slowly turning it off. CPA is fairly sensitive to heating above room temperature, so every effort was made to continuously provide cooling fluids during this process. This stage uses monofilament superconducting wire that has continuous leads to limit resistive heat generation, an issue that was observed on the PIPER mission.

Stage 2 wasn't initially thought to be undamaged, but after initial tests, it was found that the previous magnet was not able to reach it's required maximum current before quenching. Quenching occurs when the magnet suddenly goes from superconducting to normal, causing a massive and instantaneous heat load to be dumped into the ADR. Stage 2 has a diode pocket that the wires connect to before transitioning to the lead wire. This diode is present to short current and prevent damage to the winding during quenches.

The SCHS was easy to wind as epoxy is not used for this magnet, instead, Kapton tape surrounds the mandrel, keeping the wire in place. These winding were performed by the code 552 technician Tom Hait. These were the last magnet's he wound before retirement, so I was able to observe and learn the process from him, so that I can perform magnet winding's myself in the future.

3.2 Kevlar Suspensions

Kevlar is used as the suspension legs on ADRs due to their high ratio of stiffness to thermal conductivity [5]. These Kevlar strands are used in tension, Figure 6 shows the general layout.

Each side of stages 2 and 3 have three Kevlar bundles. These bundles are fed through vented 4-40 screws, wrapped around a pin and epoxied in place. The two custom nuts on the top of the suspension are used to adjust the pre-load and lock the assembly in place. In order to observe the pre-load applied on the Kevlar during assembly, a stack of four belleville washers are placed on the button head screw. These washers have a target displacement of 0.003" when the target pre-load of 8 lbf is applied. The button head screws are cut so that the bottom surface sits

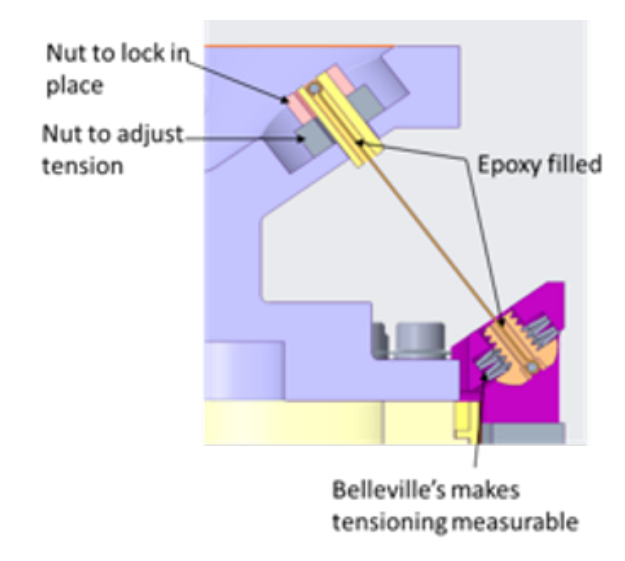


Figure 6: Kevlar Suspension Cross Section

0.003" below the surface of the fixture. Thus, we can set the pre-load by ensuring all button head screws are flush with this surface.

The pre-loading tension target of 8 lbf was found by performing Kevlar pull tests to find the strands breaking strength. 8 lbf corresponds to 30% of the Kevlar's breaking strength. This gives the assembly an adequate FOS under 8g loading conditions and provides enough stiffness to keep the strands from going slack.

When the stage has been successfully suspended, the salt-pill resides within the superconducting magnet with a 0.5 mm gap. A multimeter is used during assembly to ensure that the pill is not making contact with the magnet. This assembly limits the parasitic heating on the coldest stage to about 2.5 μ W from the 1.7 K baseplate.

3.3 Passive Gas-gap Heat Switches

The design of passive gas-gap heat switches consist of a thin titanium outer shell, with gold

plated copper fins on each side of the switch that mesh together. A 0.26 mm gap separates these fins and 3He is used to fill the void. When the heat switch is above a target temperature, these voids are completely filled, allowing heat to be conducted. When the temperature of the cold end drops below the target temperature, 3He adsorbs onto the fins, creating a vacuum and thermally isolating the two sides. The target temperature is determined by the fill pressure of 3He. Figure 7 shows a cutaway of the PGGHS's that were employed for PIPER.

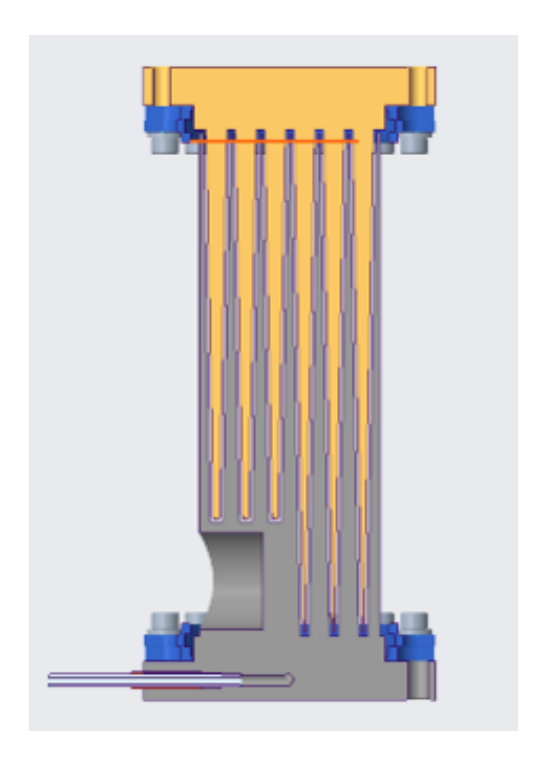


Figure 7: Passive Gas-gap Heat Switch Cross Section. Both sides of the fins are made from copper, different coloring is added to show separation.

The condition of the PGGHS's from the PIPER-EM model were unknown, therefore preliminary 'aliveness' tests were done and confirmed that the PGGHS between stage 3 and the adsorption cooler was in good condition. However, the second PGGHS was found to have a leak during our final integration test. Upon inspection, it was also found that this design was using metric threaded inserts, and these threads were damaged by mistakenly using the wrong screws. This resulted in the need to fully replace this heat switch. The new switch was then filled to 20 Torr 3He, and an additional 20 Torr of hydrogen. The hydrogen is used to increase the lifespan of the switch by preventing the 3He from getting trapped in the titanium shell, gradually lowering the on/off temp of the switch over time.

3.4 Thermal Straps

The new thermal straps that had to be designed were made from 5N pure copper. These straps were cut using wire electric discharge machining (EDM). 3D printed fixtures were used to bend the straps into their final shape, shown in Figure 8. They were then annealed at 550C for 1 hour, and gold plated.

3.5 Thermometer Calibration

Thermometers are required on each stage to allow the flight electronics to accurately control them. For this purpose, four ruthenium oxide thermometers are used, with an additional four attached for redundancy. In order to calibrate these thermometers, one calibrated and three uncalibrated thermometers were attached to a fixture shown in Figure 9, and were calibrated in parallel with the testing campaign.



Figure 8: Thermal Straps



Figure 9: Thermometer Calibration Plate

During the test, the temperature of the calibrated thermometer was controlled while measuring the resistances of the uncalibrated thermometers, shown in Figure 10. This was then used to fit equation 2 to correlate temperature and resistance. The calibrations obtained produced a curve fit error comparable to the commercially calibrated thermometer.

$$R = R_0 exp(\alpha + \frac{T_0}{T})^P + C \tag{2}$$

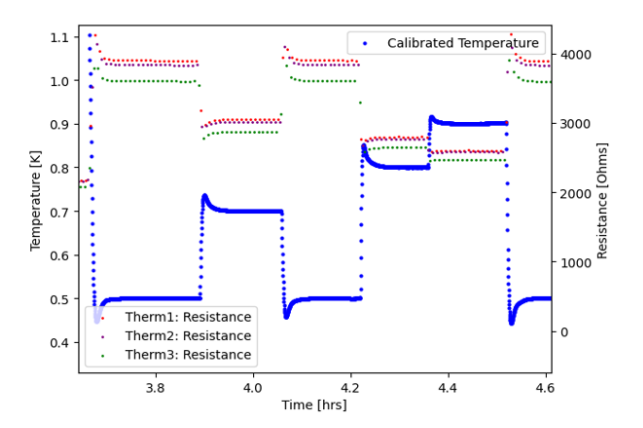


Figure 10: Thermometer Calibration Data

3.6 Assembly

The final assembly of the CADR is shown in Figure 11. High strength A286, 2-56 screws were used during assembly to decrease the thermal contact resistance as much as possible between mated components.

4 Testing and Integration

4.1 Individual Stage Testing

In parallel with the refurbishment effort, other components were tested in a cryo-cooled dewar.



Figure 11: CADR completed assembly top view (left) bottom view (right). This assembly includes the additional stage that was used to simulate the adsorption cooler during testing.

The cryocooler was able to hold a base plate temperature of 3K, and a borrowed 'upper stage' ADR was used to simulate the adsorption cooler heat sink temperature.

Over the course of a year, a total of six tests were performed on various components of the PIPER-EM model. These tests helped guide the direction of the refurbishment effort. In summary, we found all components of stage 3 to be in working order, and all components in stage 2 to be damaged. It seems possible the crash landing had a disproportionate effect on this side of the receiver, as the faulty salt pill appeared to have a 'barrel' shape possibly caused by the impact. This salt pill was replaced with a spare that was later tested and found to be working.

Alongside these tests, a need was brought forth by the branch for a better method of documenting lab data. This brought about a side project were I developed a lab note-taking software. This program simplifies the note-taking process by organizing and syncing the notes and



Figure 12: Individual Stage Testing Setup. Additional stage shown, stage being tested is mounted to the underside of the adapter plate. A PGGHS separates these two stages.

data across different computers. The software has plotting functionality built into it to allow for easy data analysis. CADR calculation libraries that I had developed for the thermal analysis were incorporated into this program to allow users to quickly calculate properties of the CADR while performing tests. This is another program that has expanded beyond use in EXCLAIM and is starting to be used by other members of the branch.

4.2 Full CADR Testing

Initial plans were to test the full 3-stage ADR in a LHe dewar. Halfway through 2022, geopolicital and economic factors made the ability to obtain LHe unfeasible for the project. This resulted in the need to pivot to a new testing setup. It was found that the CADR could potentially be tested in the same cryo-cooled dewar that used used in the individual stage tests. To make this assembly work, an additional stage was used to simulate the adsorption cooler, three new pairs of high temperature superconducting leads were installed and tested, and a new adapter plate was fabricated to integrate all the components together. Figure 13 shows the CADR fully integrated into the testing facility.



Figure 13: Assembled CADR in Test Facility

In our initial test the conductance between stages 2 and 3 was weaker than expected. This brought into question the condition of the PG-GHS connecting these stages, leading to the replacement of the heat switch, discussed in the prior section. The second test confirmed that this switch was fixed, but was showing interesting results in the temperature profile of stage 1 when the superconducting heat switch was activated. I am currently in the process of adjusting

the thermometer placement on this stage, as well ensuring the stage is well coupled to the SCHS. This appears to be the last issue to be resolved on the project.

When these tests are complete, the EXCLAIM group is going to bring the flight electronics over to the testing facility and test them with the ADR. The final test will consist of the ADR being integrated with the rest of the sub-Kelvin cooling system and tested in a LHe bath. This will conclude the testing campaign for the CADR, with the science operation expected to take place the summer of 2023.

References

- [1] P. A. R. Ade, C. J. Anderson, E. M. Barrentine, N. G. Bellis, A. D. Bolatto, P. C. Breysse, B. T. Bulcha, G. Cataldo, J. A. Connors, P. W. Cursey, N. Ehsan, H. C. Grant, T. M. Essinger-Hileman, L. A. Hess, M. O. Kimball, A. J. Kogut, A. D. Lamb, L. N. Lowe, P. D. Mauskopf, J. McMahon, M. Mirzaei, S. H. Moseley, J. W. Mugge-Durum, O. Noroozian, U. Pen, A. R. Pullen, S. Rodriguez, P. J. Shirron, R. S. Somerville, T. R. Stevenson, E. R. Switzer, C. Tucker, E. Visbal, C. G. Volpert, E. J. Wollack, and S. Yang, "The experiment for cryogenic large-aperture intensity mapping (EXCLAIM)," Journal of Low Temperature Physics, vol. 199, pp. 1027–1037, jan 2020.
- [2] E. R. Switzer, P. A. Ade, T. Baildon, D. Benford, C. L. Bennett, D. T. Chuss, R. Datta, J. R. Eimer, D. J. Fixsen, N. N. Gandilo, and et al., "Sub-kelvin cooling for two kilopixel bolometer arrays in the piper receiver," Review of Scientific Instruments, vol. 90, 2019.

- [3] Z. Szajnfarber, "The continuous adiabatic demagnetization refrigerator (cadr) innovation pathway," Massachusetts Institute of Technology, 2011.
- [4] e. a. James Tuttle, "The hawc and safire adiabatic demagnetization refrigerators," pp. 781–787.
- [5] e. a. Voellmer, George M, "A kinematic, kevlar suspension system for an adr.,"